HHS Public Access

Author manuscript

Nature. Author manuscript; available in PMC 2010 March 10.

Published in final edited form as:

Nature. 2009 September 10; 461(7261): 287–291. doi:10.1038/nature08297.

ErbB2/HER2/Neu resembles an autoinhibited invertebrate EGF receptor

Diego Alvarado, **Daryl E. Klein**, and **Mark A. Lemmon**

Department of Biochemistry and Biophysics, University of Pennsylvania School of Medicine, 809C Stellar-Chance Laboratories, 422 Curie Boulevard, Philadelphia, PA 19104-6059, U.S.A

Abstract

The orphan receptor tyrosine kinase ErbB2 (HER2/Neu) transforms cells when overexpressed1, and is an important therapeutic target in human cancer2,3. Structural studies4,5 have suggested that the oncogenic (and ligand-independent) signalling properties of ErbB2 result from the absence of a key intramolecular 'tether' in the extracellular region that autoinhibits other human ErbB receptors, including the epidermal growth factor (EGF) receptor6. Although ErbB2 is clearly unique among the four human ErbB receptors6,7, we show here that it is the closest structural relative of the single EGF receptor family member (dEGFR) in *Drosophila melanogaster*. Genetic and biochemical data show that dEGFR is tightly regulated by growth factor ligands8, yet a crystal structure shows that it too lacks the intramolecular tether seen in human EGFR, ErbB3 and ErbB4. Instead, a distinct set of autoinhibitory interdomain interactions hold unliganded dEGFR in an inactive state. All of these interactions are maintained (and even extended) in ErbB2, arguing against the suggestion that ErbB2 lacks autoinhibition. We therefore suggest that normal and pathogenic ErbB2 signalling may be regulated by ligands in the same way as dEGFR. Our findings have important implications for ErbB2 regulation in human cancer, and for developing therapeutic approaches to target novel aspects of this orphan receptor.

Ligand-induced activation of EGFR involves a dramatic change in the extracellular region from a 'tethered' (inactive) to an 'extended' (active) configuration9 (Fig. 1a) in which an exposed 'dimerization arm' in domain II drives formation of receptor dimers10,11. In tethered EGFR, the dimerization arm is occluded by autoinhibitory intramolecular interactions between domains II and IV, which are also seen in unliganded ErbB3 and ErbB4 – but are absent in ErbB26,12. ErbB2 is structurally unique. Even without a bound

Correspondence and requests for materials should be addressed to M.A.L. (e-mail: mlemmon@mail.med.upenn.edu).

Author Contributions: D.A., D.E.K. and M.A.L. conceived and designed the project. D.E.K. established initial expression and purification procedures for s-dEGFR variants and relevant ligands. D.A. was responsible for designing s-dEGFR constructs used in this study and executed all biophysical studies, crystallization, and data collection. D.A. also solved and refined the s-dEGFRΔV structure. D.A. and M.A.L. interpreted data and wrote the manuscript.

Author Information: Coordinates have been deposited in the Protein Data Bank under code 3I2T. Reprints and permissions information is available at www.nature.com/reprints.

The authors declare that they have no competing financial interests.

Full Methods and any associated references are available in the online version of the paper at www.nature.com/nature.
Supplementary Information is linked to the online version of the paper at www.nature.com/nature.

ligand its extracellular region resembles the extended (EGF-bound) form of EGFR (Fig. 1b,c), with the dimerization arm exposed and apparently 'poised' to drive receptor-receptor interactions4,5. No known soluble ligand directly regulates ErbB2, and it is the only family member that transforms cells when simply overexpressed (without ligand addition)1. Thus, ErbB2 is regarded as an 'auto-activated' receptor that adopts a constitutively activated configuration that can form signalling-active heterodimers (or homodimers) without direct growth factor regulation. These properties are thought to explain how ErbB2 overexpression causes cancer7. Although ErbB2 is viewed as an oddity among human ErbB receptors, we show here that it is the closest structural relative of the single EGF receptor family member of *D. melanogaster* (dEGFR). Moreover, the structural features that initially suggested constitutive activation of ErbB2 actually appear important for dEGFR autoinhibition. Thus, ErbB2 shares more similarities with a possible ancestral EGF receptor than does human EGFR itself.

We determined the 2.7Å X-ray crystal structure of the unliganded dEGFR extracellular region, encompassing domains I to IV (Supplementary Table 1). *D. melanogaster* contains a single EGFR/ErbB-receptor, which is tightly regulated by four different ligands (Spitz, Gurken, Keren and Vein) in distinct developmental contexts8. Ligand binding is required for dEGFR activation in cultured cells13,14 and for strong dimerization of its isolated extracellular region *in vitro*13. Sequence analyses indicate that the overall domain arrangement in dEGFR is the same as in human ErbB receptors, except for an extra cysteine-rich domain (domain V: predicted to be similar to domains II and IV) at the carboxyl terminus of the invertebrate EGFR extracellular region. Over domains I-IV (∼620 amino acids), dEGFR shares 39% sequence identity with human EGFR (hEGFR) and 35% with human ErbB2 (Supplementary Fig. 1). Because it is tightly regulated by ligands, we expected that an unliganded form of the dEGFR extracellular region (s-dEGFR) would adopt a tethered configuration similar to that seen in Fig. 1a for hEGFR. Instead, we were surprised to find that s-dEGFR encompassing domains I to IV (s-dEGFRΔV) is fully extended even in the absence of ligand (Fig. 1d), and closely resembles sErbB2 (Fig. 1c). The s-dEGFRΔV dimerization arm is exposed, and the ligand-binding sites on domains I and III are in direct contact (Fig. 1d). A structural overlay of sErbB2 and s-dEGFRΔV (Fig. 2a) shows them to be remarkably similar. Thus, the same configuration is seen for the inactive state of one ErbB receptor extracellular region (s-dEGFRΔV without ligand) and another that is thought to be constitutively active (sErbB2).

Small angle X-ray scattering (SAXS) studies excluded the possibility that crystal packing causes s-dEGFRΔV to be extended. SAXS measurements of the maximum molecular dimension (D_{max}), together with low-resolution molecular envelopes, allow clear distinction between extended and tethered configurations of ErbB receptor extracellular regions in solution15. D_{max} for s-dEGFRΔV in solution is 130Å (Supplementary Table 2), equal to the value measured for sErbB215 and 25-30Å larger than values for the tethered human EGFR extracellular region (∼105Å)15. Low-resolution molecular envelopes (Fig. 2b) also show that s-dEGFRΔV is extended in solution. SAXS studies of complete s-dEGFR (with domain V) gave an average D_{max} of 165Å (Supplementary Table 2), indicating that domain V simply projects from the end of domain IV to extend the structure (Fig. 2b and

Supplementary Fig. 2). Mutational studies provide further evidence for the absence of an autoinhibitory tether in dEGFR. The affinity of human EGFR for its ligands is increased when the domain II/IV tether is weakened with mutations or abolished by removing domain IV16,17 (Supplementary Fig. 3a). These mutations favour EGF binding by reducing the work required to relocate domains I and III for interaction with the same EGF molecule (and do not cause constitutive hEGFR activation16,18,19). Equivalent substitutions or deletions in s-dEGFR do not enhance Spitz binding (Supplementary Fig. 3b), arguing that dEGFR has no domain II/IV tether. Thus, our crystallographic and solution studies show that the unactivated *Drosophila* EGFR extracellular region adopts the same extended configuration as seen for ErbB2.

Key elements of unliganded s-dEGFR overlay very well with the unactivated human EGFR extracellular region (s-hEGFR). As shown in Fig. 3a, the conformation of domain II in inactive s-dEGFRΔV (red) closely resembles that of domain II in inactive (tethered) s-hEGFR (grey) in an overlay using domain I as reference. This appears to be a characteristic ‘inactive’ domain II conformation, which is also shared by the unliganded ErbB3 and ErbB4 extracellular regions12,20. By contrast, activated s-hEGFR11 has a strikingly different domain II structure, with a ∼12° bend between modules m4 and m5 (at the green arrow in Fig. 3b) that is known to be crucial for ligand-induced dimerization16. Importantly, the domain II conformation in sErbB2 superimposes precisely with the inactive s-dEGFR and s-hEGFR structures (cyan structure in Fig. 3a), but not with the activated human EGFR structure. ErbB2 therefore has an ‘inactive-like’ domain II, suggesting that published sErbB2 structures4,5 may actually represent an inactive (autoinhibited) configuration.

The failure of sErbB2 and unliganded s-dEGFRΔV to self-associate strongly, despite both having an exposed dimerization arm, also argues for an ‘inactive’, or dimerization-incompetent domain II conformation. The ErbB2 extracellular region does not homodimerize in solution21,22 or in crystals4,5, and its heterodimerization with other sErbB proteins is barely detectable21,22. Unliganded s-dEGFRΔV forms a crystallographic dimer mediated almost entirely by dimerization arm contacts (Supplementary Fig. 4). This self-association occurs only weakly in solution, with an approximate K_D of 40μM based on analytical ultracentrifugation experiments (Supplementary Fig. 4). Strong dimerization of s-dEGFRΔV or s-dEGFR requires Spitz binding (Supplementary Fig. 4a). Thus, the extracellular region of ErbB2 – the human ErbB receptor believed to be unique in its ability to form ligand-independent homo- and hetero-dimers7,23 – actually has less propensity for self-association than the equivalent region of the unliganded *Drosophila* EGF receptor. ErbB2 also shows no greater tendency to homodimerize in cells than unliganded hEGFR24, and is not constitutively active when expressed at physiologically relevant levels in insect cells25. Together, these data point to ErbB2 being an inactive receptor – and one that may be more stringently autoinhibited than dEGFR.

Fig. 3 suggests a mechanism for dEGFR regulation by growth factor binding that may also be relevant for ErbB2. Wedging an EGF-like molecule between the two ligand-binding domains I and III will push them apart as diagrammed in Fig. 3c, necessitating a significant bend in domain II (which links domains I and III). Movement of disulphide-bonded module m5 with respect to m4 (at the green arrow in Fig. 3b) accounts for most of this bend, and

effectively links ligand binding to reorientation of the dimerization arm. The result is a bent domain II conformation that can present a self-complementary dimerization interface (for homodimerization) or one that is optimized for heterodimerization. Direct interactions between domains I and III of s-dEGFR work against this process – and are therefore autoinhibitory. Interactions between domains I and III of s-dEGFRΔV involve regions that correspond exactly to the ligand-binding sites of hEGFR10,11, and therefore directly occlude the ligand binding sites (Fig. 1a) and bury 452 $Å^2$ of surface. Details of these interactions are shown in Supplementary Fig. 5a. The same elements in sErbB2 also contribute to direct domain I/III interactions4,5, but are augmented by additional contacts to bring domains I and III even closer together (by ∼8Å) than in s-dEGFR (Fig. 2a), burying a total surface of ∼1250$Å^2$ (Supplementary Fig. 5b). The direct domain I/III interactions seen in dEGFR (and ErbB2) are autoinhibitory because they force the two parts of the ligand-binding site so close to one another that ligand cannot be accommodated. By contrast, the domain II/IV tether in hEGFR (Fig. 1a) pulls the two halves of the ligand-binding site (on domains I and III) too far apart for them both to contact the same ligand molecule simultaneously. The autoinhibitory consequence for ligand binding is similar in both cases, with work being required to separate domains I and III in dEGFR, but (conversely) to draw them together in hEGFR by breaking the domain II/IV tether. Thus, these are variations on the same autoinhibitory theme.

The close apposition of domains I and III in dEGFR also promotes an important set of domain I/II interactions (Fig. 3c) that stabilize the inactive domain II conformation. Side-chains from the ‘back’ of s-dEGFR domain II in modules m5 and m6 (Y259 and H270 respectively) pack against a hydrophobic patch on domain I comprising the side-chains of I2, I4 and Y32 (Fig. 3c and Supplementary Fig. 6a), and form hydrogen bonds with D34 in domain I. These interactions restrain the orientation of modules m5 and m6 with respect to m4, and maintain the dimerization arm in the ‘inactive’ position shown in Fig. 3a,c. Very similar sets of domain I/II interactions occur in sErbB2 (Supplementary Fig. 6b) and inactive hEGFR (Supplementary Fig. 6c), as well as unliganded ErbB3 and ErbB412,20. All of these interactions are broken in the active configuration (Fig. 3d and Supplementary Fig. 6d), so that domain II modules m5 and m6 no longer make direct contact with domain I, and the dimerization arm becomes reoriented. Disrupting these domain I/II interactions in s-dEGFR, by mutating Y259 and H270 to alanine and serine respectively, enhances Spitz-binding to approximately the same extent as domain II/IV tether mutations enhance EGF binding to s-hEGFR17 (Supplementary Fig. 7; Supplementary Table 3). From the perspective of ligand binding, domain I/II contacts in dEGFR therefore constitute an (autoinhibitory) energetic barrier that is similar in strength to the domain II/IV tether in human EGFR, ErbB3 and ErbB4. Disrupting domain I/II contacts in intact dEGFR or ErbB2 did not elevate constitutive activity of these receptors (data not shown). Importantly, however, neither does disruption of domain II/IV tether contacts in hEGFR16,18,19. Breaking autoinhibitory interactions in the extracellular region, while necessary for activation, is clearly not sufficient. Indeed, even if domain IV is deleted entirely from s-hEGFR (so that the tether cannot form), dimerization still requires EGF addition10. Thus, the unliganded *Drosophila* and human EGF receptors rely on different sets of autoinhibitory intramolecular interactions to oppose ligand binding and dimerization.

The fact that ErbB2 maintains – and even extends – all of the autoinhibitory interactions seen in *Drosophila* EGFR argues against the prevailing notion that ErbB2 is 'poised' to dimerize through its exposed dimerization arm4,5. Furthermore, the failure of sErbB2 to form homo- or heterodimers *in vitro*21,22 suggests that it is even more stringently autoinhibited than s-dEGFR (which does homodimerize weakly) – consistent with its larger domain I/III interface (Supplementary Fig. 5). Nonetheless, crosslinking and co-immunoprecipitation studies show that intact ErbB2 can form homo- and heterodimers in mammalian cells7,23,26. One possible explanation is that ErbB2 relies uniquely on interactions outside its extracellular region to drive dimerization. A second very intriguing possibility is that unknown cellular ligands promote ErbB2 activation when it is overexpressed in mammalian cells (but not in insect cells25). The first of these possibilities is countered by reports that deleting the cytoplasmic region does not abolish ErbB2 homo- or heterodimerization26 – although a key role for the transmembrane domain cannot be excluded. The second possibility seems unlikely given the failure of substantial efforts in the 1980s and 1990s to identify direct soluble ErbB2-activating ligands7.

Although no *bona fide* soluble ligand for ErbB2 is known, at least one membrane-bound regulator that contains EGF-like domains has been identified27. A subunit of Muc4 (ASGP2) was reported to interact with ErbB2 and to promote its tyrosine phosphorylation. An EGF-like domain in membrane-associated Muc4 might bind between domains I and III of ErbB2 and induce conformational changes of the sort depicted in Fig. 3c,d to promote the ability of ErbB2 to form homo- and/or heterodimers. Intriguingly, it has been shown genetically that Spitz must be palmitoylated (which drives its membrane association28) in order to regulate dEGFR *in vivo*28. Gurken and Keren have a similar palmitoylation site, whereas Vein – considered to be a 'weak' dEGFR ligand8 – does not. Thus, membrane association appears to be a key feature of ligands (Muc4 and Spitz) that activate the two ErbB receptors known to adopt an extended configuration in the absence of ligand (ErbB2 and dEGFR). Membrane association may be required to increase the local ligand concentration at the cell surface, so as to promote the ligand's ability to 'wedge apart' domains I and III of dEGFR or ErbB2 (breaking autoinhibitory domain I/III interactions). By contrast, the tethered configuration of hEGFR, ErbB3 and ErbB4 (Fig. 1a) keeps the ligand-binding sites on domains I and III fully exposed and freely accessible to soluble growth factors. We speculate that evolution of the domain II/IV tether as a distinct mode of autoinhibition might have occurred alongside the ability of ErbB receptors (other than ErbB2) to respond to soluble (rather than membrane-bound) growth factor ligands.

Given the importance of ErbB2 in human cancer, and its validated utility as a target of cancer therapeutics3, the view of ErbB2 regulation presented here has several implications. Developing agents that stabilize autoinhibitory interactions might represent a new therapeutic avenue for inhibiting ErbB2 signalling in cancer. Just as importantly, the fact that ErbB2 shows such striking resemblance to a tightly ligand-regulated invertebrate EGF receptor argues that ErbB2 also has activating ligands. Identifying these likely membrane-associated ligands, and appreciating their role in activating ErbB2 in different human cancers, should provide important new directions for therapeutic targeting of ErbB receptor signalling.

Methods Summary

Histidine-tagged s-dEGFR and s-dEGFRΔV were produced by secretion from baculovirus-infected *Spodoptera frugiperda* Sf9 cells or transfected *Drosophila* S2 cells. The C-terminal amino acid of s-dEGFRΔV was T589 in the numbering convention used in Supplementary Fig. 1 (see Online Methods). Secreted protein was harvested by metal affinity chromatography, and further purified by ion exchange and size-exclusion chromatography as described13. Surface plasmon resonance (SPR), small angle X-ray scattering (SAXS) and sedimentation equilibrium analytical ultracentrifugation studies were performed essentially as described13,15,16.

Purified s-dEGFRΔV was crystallized using the vapour diffusion method in 10% PEG 4000, 5% Jeffamine M-600 (pH 7.0), 12.5% ethylene glycol, 100mM HEPES, pH 7.4, and 50mM KCl. Plate-shaped crystals of approximate dimensions 200μm × 200μm × 75μm grew in 1-5 days, and were frozen directly from the mother liquor. Data were collected using beamline 23ID-D at the Advanced Photon Source (Argonne, IL), as described in Supplementary Table 1. The structure of s-dEGFRΔV was solved using molecular replacement (MR) methods. Search models based on the coordinates of domains I and III from ErbB2 (PDB code 2a91)5 were generated by substituting non-conserved amino acids with alanines. Although MR solutions could not be found for domains II or IV, initial maps based on domain I/III models showed strong density for domain II. Model building with COOT29, was alternated with successive rounds of restrained refinement using REFMAC30. In later stages of refinement, composite omit maps were generated, which allowed much of domain IV to be built, and oligosaccharides to be placed.

Online Methods

Protein expression and purification

Coding regions for wild-type and mutated forms of s-dEGFR were subcloned into pFastbac-1 and pMT/V5-His A (Invitrogen) for expression in *Spodoptera frugiperda* (Sf9) and *Drosophila melanogaster* Schneider-2 (S2) cells respectively. A C-terminal hexa-histidine tag was incorporated in all constructs using PCR. s-dEGFRΔV ended at T589 using the numbering scheme employed in Supplementary Fig. 1 (see comments in Crystallography section below on dEGFR numbering), and s-dEGFRΔIV-V was truncated at N493. Two sets of mutations were made to disrupt the domain I/II autoinhibitory interface for Supplementary Fig. 7 and Supplementary Table 3. In one, Y259 and H270 in domain II were mutated to alanine and serine respectively. In the second, sites in domains I and II were mutated, to give the tetramutant I2A/Y32A/Y259A/H270S. The effects of these mutations were assessed both in the background of wild-type s-dEGFR and a Y242S/Y247S mutant in which dimer contacts are disrupted. The s-dEGFRΔV$^{dim\text{-}arm}$ construct referred to in Supplementary Fig. 4 and Supplementary Table 2 contains a series of mutations in the domain II dimerization arm analogous to those previously shown to abolish ligand-induced dimerization of human sEGFR10: Y242E, N243A, T245D, Y247E, V248A, and L249D. The s-dEGFR^{tether} mutant referred to in Supplementary Fig. 3 contains three mutations in domain IV analogous to those that break all intramolecular hydrogen-bonding interactions between domains II and IV observed in the unliganded s-hEGFR structure17: D547A,

H550A, and K559A. All mutations were generated using the QuikChange mutagenesis kit (Stratagene) and fully sequenced.

Stable S2 cell pools and recombinant baculoviruses were generated as described13,17,31, and each protein of interest was secreted into the culture medium. For S2 cell-expressed proteins, S2 cells were grown in EX-CELL 420 serum-free medium (Sigma-Aldrich) to a density of ∼5-10×106 cells/ml, and protein expression was induced with 500 μM $CuSO_4$ for 3-4 days. For Sf9 cell-expressed proteins, Sf9 cells were grown in Sf900II medium (Invitrogen-Gibco) to a density of 2-3×10^6 cells/ml, and were infected with recombinant baculovirus for 3-4 days. In each case, 2-4 litres of conditioned media were flowed over a 3-4 ml bed volume of Ni-NTA agarose (Qiagen). After washing the column with 25mM MES pH 6.0, 150mM NaCl (buffer A), bound proteins were eluted with increasing concentrations of imidazole in buffer A. Protein-containing fractions were applied to a Uno-S (Biorad) cation-exchange column, equilibrated in buffer A, and were eluted with a salt gradient from 150mM to 1M NaCl in buffer A. s-dEGFR proteins eluted between 200-500mM NaCl, and were concentrated using a Centricon-50 concentrator (Millipore) prior to further purification with size exclusion chromatography using a Superose-6 column (GE Healthcare) equilibrated in buffer B (25mM HEPES pH 8.0, 150mM NaCl). Secreted Spitz and $Spitz^{C29S}$ were purified from S2 cells exactly as described previously13,28,31.

Surface Plasmon Resonance (SPR)

Secreted Spitz was immobilized onto CM5 sensorchips using amine coupling, exactly as described previously13. Increasing concentrations of s-dEGFR proteins (12.5nM - 6,400nM) were then flowed over the sensorchip in buffer B containing 0.005% Surfactant P20 at 25°C. The sensorchip surface was regenerated after each injection using 10mM sodium acetate, pH 4.5, 1M NaCl, as described13. The maximum SPR response at steady state for each s-dEGFR concentration was plotted against s-dEGFR concentration, and the resulting curves could be fit straightforwardly to simple binding isotherms using the program Prism (GraphPad), from which apparent K_D values were obtained. Standard error of the mean (S.E.M) values were generated from at least 3 independent measurements, using at least two independent preparations of each protein.

Small angle X-ray scattering (SAXS)

SAXS data were collected at room temperature both with a rotating anode source at Fox Chase Cancer Center (courtesy of Dr. Zimei Bu), as described15, or at CHESS beamline G1, using protein samples at concentrations between 1-6 mg/ml in buffer B. Data handling and reduction were performed as described previously15 or using the program Datasqueeze (Datasqueeze Software). Potential problems with radiation-induced denaturation were monitored by inspection of Kratky plots with increasing exposure time, graphing IQ^2 as a function of Q, where I is the scattered intensity and $Q=4\pi\sin(\theta/2)/\lambda$ (where Q is the magnitude of the scattering vector, with θ as the scattering angle and λ as the X-ray wavelength). The program GNOM32 was used to obtain $P(r)$ curves, the maximum dimension of the molecule (D_{max}), and its radius of gyration (R_g). Quoted R_g values (Supplementary Table 2) represent means (± standard deviation) from at least three independent determinations. D_{max} values were determined empirically by recomputing $P(r)$

curves in GNOM using a series of different r_{max} values (in steps of 5Å), and selecting as D_{max} the r_{max} value at which $P(r)$ most closely approached zero while giving a plausible $P(r)$ curve. Errors in D_{max} values are quoted as ±5Å based on the empirical approach used for their determination. Low-resolution molecular envelopes were generated *ab initio* using the program DAMMIN as previously described16,17,33, using SAXS data collected on the home source with s-dEGFR concentrations between 1-2 mg/ml. Briefly, ten iterations of DAMMIN were averaged and filtered as described34, using the DAMAVER suite of programs. Crystal structures of models were docked into the resulting 'most probable' envelopes using SITUS35, and the outputs were displayed and manually refined using the UCSF Chimera package (http://www.cgl.ucsf.edu/chimera)36.

Sedimentation equilibrium ultracentrifugation

Experiments were performed exactly as described21, with the following modifications. Receptor extracellular regions at 2, 4, and 8μM, both with- and without a 1.2-fold excess of Spitz were centrifuged in buffer B at 6,000, 9,000, and 12,000 rpm in an Optima XL-A analytical ultracentrifuge (Beckman) at 25°C, using absorbance at 280nm to detect protein distribution. The program Winmatch (http://www.biotech.uconn.edu/auf/) was utilized to ensure that samples had reached equilibrium. Data were analyzed using Sedfit and Sedphat (http://www.analyticalultracentrifugation.com), and were fit to a monomer-dimer equilibrium model as described16, considering s-dEGFR or the s-dEGFR/Spitz complex as the dimerizing species. Fits used to determine the quoted K_D values gave good residuals, with no systematic deviations. In Supplementary Fig. 4a, sedimentation data are plotted as $\ln A_{280}$ vs. $(r^2\text{-}r_0^2/2)$, where r is the radial position in the sample and r_o is the radial position of the meniscus. For a single species, this representation gives a straight line with slope proportional to its molecular mass. Standard deviations quoted represent data from at least three independent experiments.

Crystallography

Generation of s-dEGFRΔV protein suitable for crystallization

The *torpedo* locus in *Drosophila melanogaster* encodes two splice variants named dEGFR1 and dEGFR2 that differ only at their N-termini37,38. Mature dEGFR1 and dEGFR2 have N-terminal extensions of 21 and 71 amino acids respectively, which show no significant sequence similarity, are devoid of significant predicted secondary structure, and are proteolytically labile as determined by N-terminal sequencing of the corresponding s-dEGFR species. We found that s-dEGFR1 and s-dEGFR2 bind Spitz with the same affinity (data not shown), and removal of the N-terminal extensions has no influence on Spitz binding (data not shown). Beyond amino acid 22 of mature dEGFR1 (C53 of predicted pro-dEGFR1) and amino acid 72 of mature dEGFR2 (C102 of pro-dEGFR2), the two splice-forms are identical. Therefore, to generate a protein amenable for crystallization (s-dEGFR), we deleted amino acids 1-21 and 1-71 of mature dEGFR1 and dEGFR2 respectively (equivalent to amino acids 1-52 and 1-101 of the respective pro-forms), so that the N-terminal amino acid of mature s-dEGFR corresponds to K20 of mature dEGFR1 or K70 of mature dEGFR2 (the second residue: V21 in mature dEGFR1 and I71 in mature dEGFR2, is I2 in mature s-dEGFR: Supplementary Fig. 1). Immediately before K1 of s-dEGFR, we

added a BiP signal sequence (substituted for the native one) to drive secretion of s-dEGFR into the culture medium, followed by a hexahistidine tag (in addition to the His_6 tag at the C-terminus), so that the presumed mature s-dEGFR protein secreted from S2 or Sf9 cells starts with six histidines, which we number -5 to 0. Domain V was also deleted from s-dEGFR at Thr 589 (using the numbering in Supplementary Fig. 1), yielding s-dEGFRΔV, which also has a C-terminal hexa-histidine tag. Whereas crystals grown with s-dEGFR2 protein diffracted poorly, s-dEGFRΔV crystals diffracted well to 2.7Å resolution.

Crystallization and data collection

Purified s-dEGFRΔV (see above) at 100μM was crystallized using the vapour diffusion method by mixing equal volumes of protein with a solution containing 10% PEG 4000, 5% Jeffamine M-600 (pH 7.0), 12.5% ethylene glycol, 100mM HEPES, pH 7.4, and 50mM KCl, and equilibrating the mixture over a reservoir of this solution at 21°C. Plate-shaped crystals of approximate dimensions 200μm × 200μm × 75μm grew in 1-5 days, and were frozen directly from the mother liquor. Data were collected using beamline 23ID-D at the Advanced Photon Source (Argonne, IL), and were processed using HKL-200039. Crystals were of space group $C222_1$, with unit cell dimensions a=74.4Å, b=174.8Å, c=161.6Å and α=β=γ=90°. There is one s-dEGFRΔV molecule in the asymmetric unit, with a Matthews coefficient of 3.2$Å^3$/Da, giving a solvent content of 62.2%.

Molecular replacement and refinement

The structure of s-dEGFRΔV was solved using molecular replacement (MR) methods. Search models based on the coordinates of domains I and III from ErbB2 (PDB code 2a91)10 were generated by substituting non-conserved amino acids with alanines. Domains I and III were found in simultaneous but independent searches using PHASER (CCP4)30. Although we were unable to find MR solutions for domains II or IV with a variety of search models, initial maps based on domain I/III models showed strong density for domain II. Model building with COOT29, was alternated with successive rounds of restrained refinement using REFMAC30, and solvent flattening with DM30. In later stages of refinement, composite omit maps were generated in CNS40, which allowed much of domain IV to be built, and oligosaccharides to be placed. The final stages of refinement employed TLS refinement41 with anisotropic motion tensors refined for each of the four domains, using REFMAC30.

Calculations and figure preparation

Calculations of buried surface were performed using AREAIMOL in the CCP4 suite of programs30. Calculations of surface complementarity,S_C42 used the program SC in CCP430. Structure validation was performed with SFCHECK and PROCHECK in CCP430. Figures were generated using MacPymol43 (http://www.pymol.org).

Supplementary Material

Refer to Web version on PubMed Central for supplementary material.

Acknowledgments

We thank members of the Lemmon and Ferguson laboratories, Kathryn Ferguson, Greg Van Duyne, Charles Abrams, and Jim Shorter for advice and comments on the manuscript. We thank Zimei Bu, at Fox Chase Cancer Center, for assistance with collecting SAXS data, and Dr. Richard Gillilan of MacCHESS for help with SAXS data collection and processing at CHESS beamline G1. Crystallographic results were obtained in research conducted at the GM/CA Collaborative Access Team at the Advanced Photon Source (APS), supported with funds from the National Cancer Institute and National Institute of General Medical Science. Supported by grants from the NIH (to M.A.L.). D.E.K. was supported by a Predoctoral fellowship from the U.S. Army Breast Cancer Research Program. D.A. was supported by an NIH Postdoctoral Training Grant and a Postdoctoral Fellowship from the Damon Runyon Cancer Research Foundation.

References

1. Di Fiore PP. erbB-2 is a potent oncogene when overexpressed in NIH/3T3 cells. Science. 1987; 237:178–182. [PubMed: 2885917]
2. Hynes NE, Lane HA. ERBB receptors and cancer: the complexity of targeted inhibitors. Nat Rev Cancer. 2005; 5:341–354. [PubMed: 15864276]
3. Moasser MM. Targeting the function of the HER2 oncogene in human cancer therapeutics. Oncogene. 2007; 26:6577–6592. [PubMed: 17486079]
4. Cho HS, et al. Structure of the extracellular region of HER2 alone and in complex with the Herceptin Fab. Nature. 2003; 421:756–760. [PubMed: 12610629]
5. Garrett TP, et al. The crystal structure of a truncated ErbB2 ectodomain reveals an active conformation, poised to interact with other ErbB receptors. Mol Cell. 2003; 11:495–505. [PubMed: 12620236]
6. Burgess AW, et al. An open-and-shut case? Recent insights into the activation of EGF/ErbB receptors. Mol Cell. 2003; 12:541–552. [PubMed: 14527402]
7. Citri A, Skaria KB, Yarden Y. The deaf and the dumb: the biology of ErbB-2 and ErbB-3. Exp Cell Res. 2003; 284:54–65. [PubMed: 12648465]
8. Shilo BZ. Regulating the dynamics of EGF receptor signaling in space and time. Development. 2005; 132:4017–4027. [PubMed: 16123311]
9. Lemmon MA. Ligand-induced ErbB receptor dimerization. Exp Cell Res. 2009; 315:638–648. [PubMed: 19038249]
10. Garrett TP, et al. Crystal structure of a truncated epidermal growth factor receptor extracellular domain bound to transforming growth factor alpha. Cell. 2002; 110:763–773. [PubMed: 12297049]
11. Ogiso H, et al. Crystal structure of the complex of human epidermal growth factor and receptor extracellular domains. Cell. 2002; 110:775–787. [PubMed: 12297050]
12. Bouyain S, Longo PA, Li S, Ferguson KM, Leahy DJ. The extracellular region of ErbB4 adopts a tethered conformation in the absence of ligand. Proc Natl Acad Sci U S A. 2005; 102:15024–15029. [PubMed: 16203964]
13. Klein DE, Nappi VM, Reeves GT, Shvartsman SY, Lemmon MA. Argos inhibits epidermal growth factor receptor signalling by ligand sequestration. Nature. 2004; 430:1040–1044. [PubMed: 15329724]
14. Schweitzer R, Shaharabany M, Seger R, Shilo BZ. Secreted Spitz triggers the DER signaling pathway and is a limiting component in embryonic ventral ectoderm determination. Genes Dev. 1995; 9:1518–1529. [PubMed: 7601354]
15. Dawson JP, Bu Z, Lemmon MA. Ligand-induced structural transitions in ErbB receptor extracellular domains. Structure. 2007; 15:942–954. [PubMed: 17697999]
16. Dawson JP, et al. Epidermal growth factor receptor dimerization and activation require ligand-induced conformational changes in the dimer interface. Mol Cell Biol. 2005; 25:7734–7742. [PubMed: 16107719]
17. Ferguson KM, et al. EGF activates its receptor by removing interactions that autoinhibit ectodomain dimerization. Mol Cell. 2003; 11:507–517. [PubMed: 12620237]

18. Mattoon D, Klein P, Lemmon MA, Lax I, Schlessinger J. The tethered configuration of the EGF receptor extracellular domain exerts only a limited control of receptor function. Proc Natl Acad Sci USA. 2004; 101:923–928. [PubMed: 14732693]
19. Walker F, et al. CR1/CR2 interactions modulate the functions of the cell surface epidermal growth factor receptor. J Biol Chem. 2004; 279:22387–22398. [PubMed: 15016810]
20. Cho HS, Leahy DJ. Structure of the extracellular region of HER3 reveals an interdomain tether. Science. 2002; 297:1330–1333. [PubMed: 12154198]
21. Ferguson KM, Darling PJ, Mohan MJ, Macatee TL, Lemmon MA. Extracellular domains drive homo- but not hetero-dimerization of erbB receptors. EMBO J. 2000; 19:4632–4643. [PubMed: 10970856]
22. Horan T, et al. Binding of Neu differentiation factor with the extracellular domain of Her2 and Her3. J Biol Chem. 1995; 270:24604–24608. [PubMed: 7592681]
23. Penuel E, Akita RW, Sliwkowski MX. Identification of a region within the ErbB2/HER2 intracellular domain that is necessary for ligand-independent association. J Biol Chem. 2002; 277:28468–28473. [PubMed: 12000754]
24. Wehrman TS, et al. A system for quantifying dynamic protein interactions defines a role for Herceptin in modulating ErbB2 interactions. Proc Natl Acad Sci USA. 2006; 103:19063–19068. [PubMed: 17148612]
25. Berger MB, Mendrola JM, Lemmon MA. ErbB3/HER3 does not homodimerize upon neuregulin binding at the cell surface. FEBS Lett. 2004; 569:332–336. [PubMed: 15225657]
26. Brennan PJ, Kumagai T, Berezov A, Murali R, Greene MI. HER2/neu: mechanisms of dimerization/oligomerization. Oncogene. 2000; 19:6093–6101. [PubMed: 11156522]
27. Carraway KL, Ramsauer VP, Haq B, Carothers Carraway CA. Cell signaling through membrane mucins. Bioessays. 2003; 25:66–71. [PubMed: 12508284]
28. Miura GI, et al. Palmitoylation of the EGFR ligand Spitz by Rasp increases Spitz activity by restricting its diffusion. Dev Cell. 2006; 10:167–176. [PubMed: 16459296]
29. Emsley P, Cowtan K. Coot: model-building tools for molecular graphics. Acta Crystallogr D Biol Crystallogr. 2004; 60:2126–2132. [PubMed: 15572765]
30. CCP4 (Collaborative Computational Project Number 4). The CCP4 suite: Programs for protein crystallography. Acta Crystallogr D Biol Crystallogr. 1994; 50:760–763. [PubMed: 15299374]
31. Klein DE, Stayrook SE, Shi F, Narayan K, Lemmon MA. Structural basis for EGFR ligand sequestration by Argos. Nature. 2008; 453:1271–1275. [PubMed: 18500331]
32. Svergun DI. Determination of the Regularization Parameter in Indirect-Transform Methods Using Perceptual Criteria. J Appl Crystallogr. 1992; 25:495–503.
33. Svergun DI. Restoring low resolution structure of biological macromolecules from solution scattering using simulated annealing. Biophys J. 1999; 76:2879–2886. [PubMed: 10354416]
34. Volkov VV, Svergun DI. Uniqueness of ab initio shape determination in small-angle scattering. J Appl Cryst. 2003; 36:860–864.
35. Wriggers W, Birmanns S. Using situs for flexible and rigid-body fitting of multiresolution single-molecule data. J Struct Biol. 2001; 133:193–202. [PubMed: 11472090]
36. Pettersen EF, et al. UCSF Chimera--a visualization system for exploratory research and analysis. J Comput Chem. 2004; 25:1605–1612. [PubMed: 15264254]
37. Clifford R, Schupbach T. Molecular analysis of the Drosophila EGF receptor homolog reveals that several genetically defined classes of alleles cluster in subdomains of the receptor protein. Genetics. 1994; 137:531–550. [PubMed: 8070664]
38. Lesokhin AM, Yu SY, Katz J, Baker NE. Several levels of EGF receptor signaling during photoreceptor specification in wild-type, Ellipse, and null mutant Drosophila. Dev Biol. 1999; 205:129–144. [PubMed: 9882502]
39. Otwinowski Z, Minor W. Processing of X-ray diffraction data collected in oscillation mode. Methods Enzymol. 1997; 276:307–326.
40. Brunger AT, et al. Crystallography & NMR system: A new software suite for macromolecular structure determination. Acta Crystallogr D Biol Crystallogr. 1998; 54:905–921. [PubMed: 9757107]

41. Winn MD, Isupov MN, Murshudov GN. Use of TLS anisotropic displacements in macromolecular refinement. Acta Crystallogr D Biol Crystallogr. 2001; 57:122–133. [PubMed: 11134934]
42. Lawrence MC, Colman PM. Shape complementarity at protein/protein interfaces. J Mol Biol. 1993; 234:946–950. [PubMed: 8263940]
43. DeLano, WL. The PyMOL Molecular Graphics System. DeLano Scientific; Palo Alto, CA, USA: 2002.

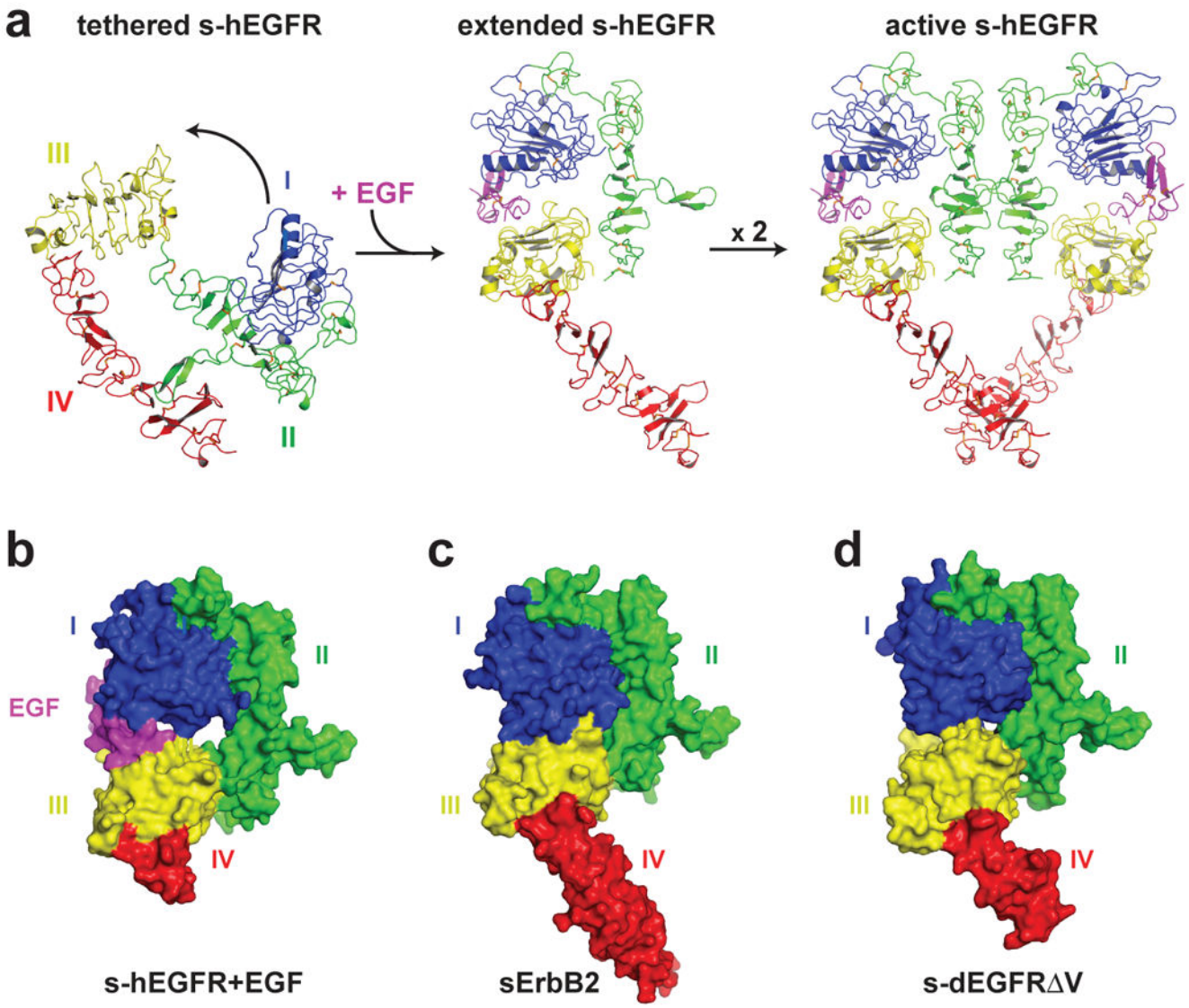

Figure 1.

ErbB receptor autoinhibition.

a, The unliganded hEGFR extracellular region adopts a tethered structure (left), burying its dimerization arm (green) in autoinhibitory domain II/IV interactions. Domains I, II, III and IV are blue, green, yellow and red respectively. Binding of EGF (magenta) to domains I and III stabilizes extended s-hEGFR, exposing the dimerization arm (centre) to promote receptor dimerization (right)9. Most of domain IV was missing from extended s-hEGFR10,11 structures, and was added to the centre and right-hand panels using the domain IV structure of tethered s-hEGFR (left)17. **b**, Surface representation of a monomer from the EGF-bound s-hEGFR dimer (PDB ID 1ivo)11. **c**, sErbB2 (PDB ID 1n8z: shown in surface representation) adopts an extended configuration similar to an activated s-hEGFR monomer4. **d**, Even in its inactive, unliganded state, s-dEGFRΔV is completely extended and closely resembles both sErbB2 and activated s-hEGFR.

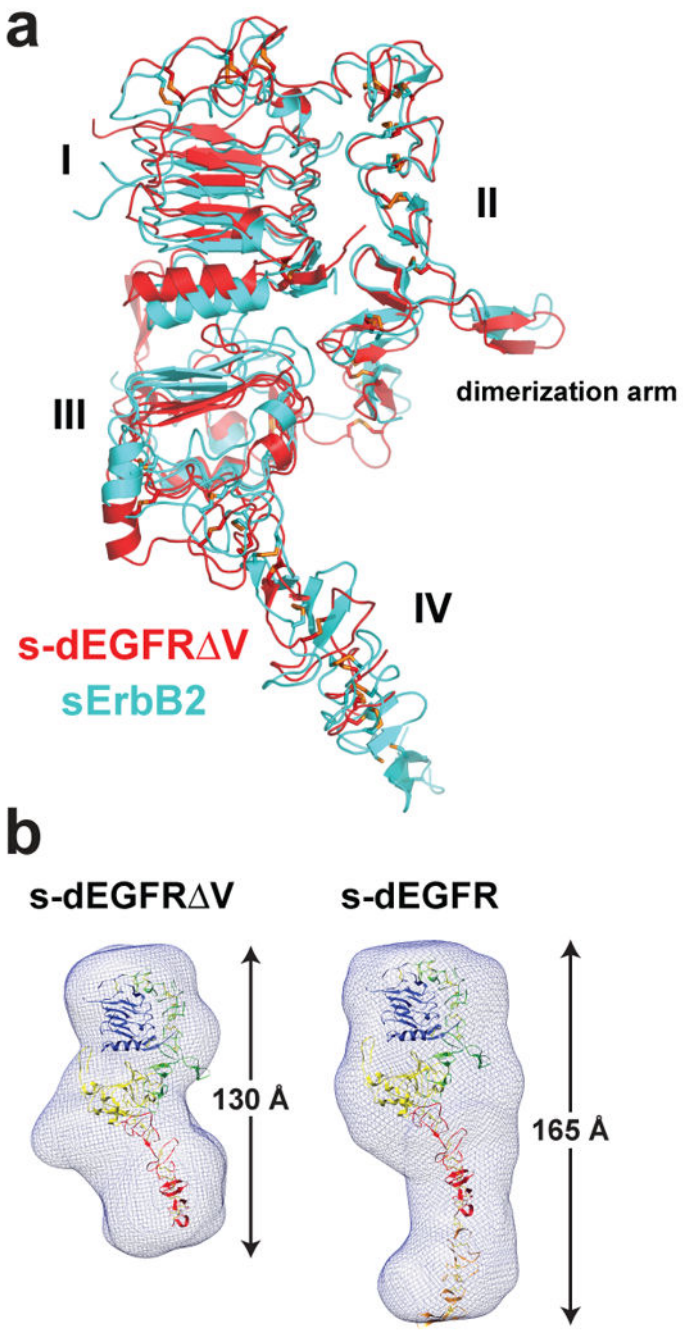

Figure 2.

The unactivated dEGFR extracellular region closely resembles sErbB2.

a, Global superimposition of inactive s-dEGFRΔV (red) and sErbB2 (cyan)4 illustrates their conformational similarity. Direct domain I-III interactions (more extensive in sErbB2 than in s-dEGFR) help stabilize the extended configuration in both receptors (Supplementary Fig. 5) and block ligand-binding sites.

b, Low-resolution molecular envelopes from small-angle X-ray scattering (SAXS) studies of s-dEGFRΔV (left) and s-dEGFR (right), with maximum molecular dimensions (D_{max})

marked (see Supplementary Table 2). The s-dEGFRΔV envelope readily accommodates the crystallographic model. In intact s-dEGFR, domain V (orange) appears simply to add to the maximum dimension. Domain V and the domain IV C-terminus (poorly defined in our crystal structure) were modelled using s-hEGFR domain IV as template. In the right-hand panel, the three most C-terminal terminal disulphide-linked modules of domain V have been removed. The fact that these are not accommodated by the SAXS envelope suggests flexibility at the C-terminus.

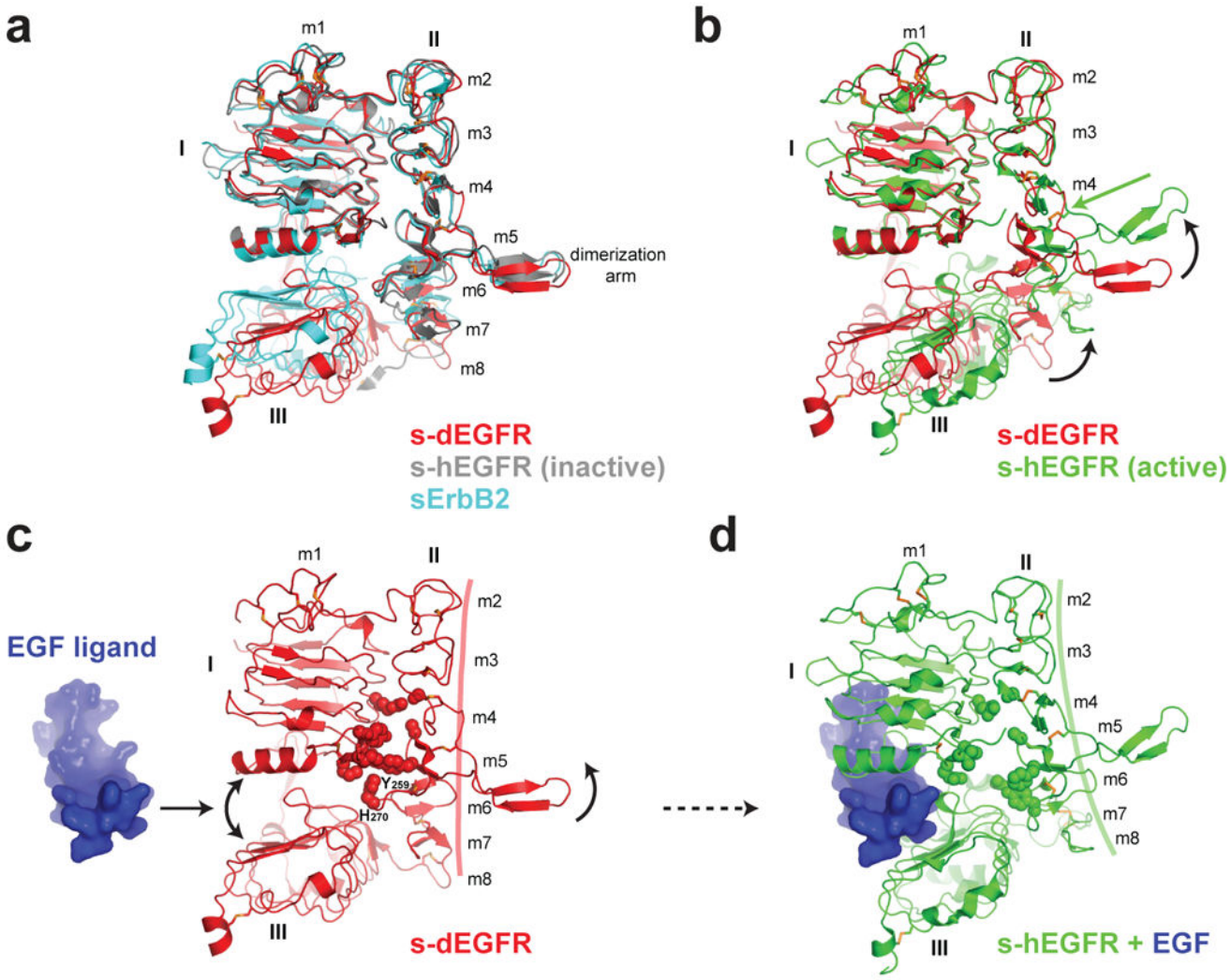

Figure 3.

Ligand binding breaks autoinhibitory domain I/II interactions common to s-dEGFR, s-hEGFR and sErbB2.

a, Superposition of inactive s-hEGFR (grey) on s-dEGFRΔV (red) and sErbB2 (cyan) using domain I as reference. The eight disulphide-bonded modules (m1-m8) that define domain II are labelled, as is the dimerization arm – located almost identically in all three structures. Domain III of inactive s-hEGFR is removed for clarity. **b**, A similar overlay of active s-hEGFR (green) and inactive s-dEGFRΔV (red) highlights dimerization arm reorientation upon ligand binding. The structures overlay very well in modules m1-m4 of domain II, but deviate significantly at the m4/m5 linkage (green arrow) because of a ligand-induced bend. **c-d**, Model for activation of dEGFR (and ErbB2) by wedging an EGF-like ligand (blue) between domains I and III. Forcing domains I and III apart disrupts all direct domain I/III interactions, as well as a set of domain I/II contacts that normally maintain domain II in an inactive conformation (residues shown in space-filling representation: see Supplementary

Fig. 6). In EGF-bound s-hEGFR (**d**), the side-chains shown in green space-filling representation no longer interact, and domain II is bent.